Numerical Simulation and Analysis of a Vertical Centrifuge

Chuan Wang, Chi Huang and Huachuan Liu

School of Southwest Petroleum University, Sichuan 610000, China

Abstract

In order to solve the separation efficiency problem of the vertical centrifuge. First, understand the working principle and dynamic theory of the centrifuge, preliminarily design the technical parameters from the experience and experimental data of the prototype, solid works model, specify the overall structure scheme, and complete the virtual assembly. Secondly, the work performance is verified. The production capacity is calculated with power to meet the design requirements. Then, to verify the design strength and deformation meet the design requirements. Then, the finite element numerical analysis of the internal flow field. The FLUENT software is used to analyze the internal flow field velocity distribution and the turbulent kinetic energy of the centrifuge. Finally, a solid phase distribution rule analysis was performed to investigate the effect of particle diameter size on the separation performance at a suitable particle volume fraction.

Keywords

Vertical Centrifuge; FLUENT; Analysis of the Internal Flow file.

1. Foreword

At present, the domestic in the design of horizontal screw centrifuge and research has obtained rich theoretical research results and good practical application value, this paper on the basis of the reference of horizontal centrifuge design ideas, in the overall structure design of centrifuge, technical parameters optimization, and stepless speed regulation, the ultimate goal is to solve the problem of separation efficiency of centrifuge. The technical indexes of the vertical centrifuge developed in this paper are:

- (1) Maximum rotation speed: 3,000 r / min
- (2) Centrifugation effect: 3,000
- (3) Main motor (kw): 18.5~30
- (4) Differential motor (kw): 18.5~30
- (5) Centrifuge processing capacity: 0m³/h~3m³/h

Compared with similar centrifuges, the prototype has high separation factor, small size solid separation, and adapt to the difficult separation; the slag diameter is large, the sediment directly out of the drum, generally will not appear slag blocking phenomenon; the technical parameters are optimized with multiple objectives, the material torque and axial force is relatively small, the slag efficiency is guaranteed, speed regulation is simple and convenient.

In 2004, Sun Bugong designed a cement sand separator for the high sediment flow of the Yellow River. In order to make the Yellow River water without sediment or a little sediment flow into the drip irrigation system, Sun Bugong introduced the separation principle of the disc centrifuge, and calculated the main structural parameters of the disc centrifuge, including the thickness of the drum wall, the inner and outer diameter of the disc, the disc gap, the height of the disc bundle, the cone corner of the disc bus, etc. And performed the estimation of the power and separation performance of the centrifuge. In the process of the prototype, the vibration is discussed and the dynamic balance method of the disc centrifuge.

In 2019, wang jiing for most domestic manufacturers and customers need different flow of centrifugal compressor to meet the requirements of the new conditions and reduce labor costs, wang jiing in the original centrifugal compressor impeller model, according to the demand of different flow level, using S OLIDWORKS centrifugal blade three dimensional modeling, to get the fluid part of the domain, and then use CFD software numerical calculation analysis.

2. Theoretical Method of Numerical Analysis

Computational fluid dynamics (Computational Fluid Dynamics, CFD) is a discipline that uses numerical methods to solve the basic equation of fluid mechanics, so as to obtain the discrete quantitative description of the flow field, and to predict the motion law of the fluid. The basic idea of CFD can be summarized as: the original in the space domain and time domain continuous physical quantity of the field, such as flow field, temperature field and pressure field, with finite discrete point set of variable value instead, through certain relationship about the variables between the mathematical equations, and then solve the equation system of the variables.

1. Quality conservation equation

For microelements fixed in space, the law of conservation of mass can be expressed as: the increase of fluid mass in the microelement per unit time = the net mass flowing into the microelement at intervals in the same time. Any flow problem must satisfy the law of conservation of mass. By this law, the mass conservation equation, the continuous equation.

The increase rate of quality per unit time is:

$$\frac{\partial}{\partial t} (\rho \delta x \delta y \delta z) = \frac{\partial \rho}{\partial t} \delta x \delta y \delta z \tag{1}$$

The mass flow through the boundary is:

$$\left(\rho u - \frac{\partial(\rho u)}{\partial x} \frac{\partial x}{2}\right) \partial y \partial z - \left(\rho u + \frac{\partial(\rho u)}{\partial x} \frac{\partial x}{2}\right) \partial y \partial z + \left(\rho v - \frac{\partial(\rho v)}{\partial y} \frac{\partial y}{2}\right) \partial x \partial z - \left(\rho v + \frac{\partial(\rho v)}{\partial y} \frac{\partial y}{2}\right) \partial x \partial z + \left(\rho w - \frac{\partial(\rho w)}{\partial z} \frac{\partial z}{2}\right) \partial x \partial y - \left(\rho w + \frac{\partial(\rho w)}{\partial z} \frac{\partial z}{2}\right) \partial x \partial y$$

$$\left(\rho w - \frac{\partial(\rho w)}{\partial z} \frac{\partial z}{2}\right) \partial x \partial y - \left(\rho w + \frac{\partial(\rho w)}{\partial z} \frac{\partial z}{2}\right) \partial x \partial y$$
(2)

The mass conservation equation can be obtained as follows:

$$\frac{\partial \rho}{\partial t} + \frac{\partial (\rho u)}{\partial x} + \frac{\partial (\rho v)}{\partial y} + \frac{\partial (\rho w)}{\partial z} = 0$$
(3)

Add the vector symbol div (a) = formula $\frac{\partial a_x}{\partial x} + \frac{\partial a_y}{\partial y} + \frac{\partial a_z}{\partial z} + \frac{\partial (\rho u)}{\partial t} + \frac{\partial (\rho u)}{\partial x} + \frac{\partial (\rho v)}{\partial y} + \frac{\partial (\rho w)}{\partial z} = 0$

(2.3) The mass conservation equation can be expressed as:

$$\frac{\partial \rho}{\partial t} + div(\rho u) = 0 \tag{4}$$

In the above equation, the —— density $^{\rho}$

t—— time

u—— velocity vector

Given above is the mass equation for the transient three-dimensional compressible fluid. If the flow is in steady state and the fluid is homogeneous and incompressible, the density ρ is constant, it can be expressed as:

$$\frac{\partial u}{\partial x} + \frac{\partial v}{\partial y} + \frac{\partial w}{\partial z} = 0 \tag{5}$$

2. Momentum conservation equation

The law of conservation of momentum is also a fundamental law that must be satisfied by any flow system. The law can be expressed as: the increase rate of the fluid momentum in the microelement body = the sum of the various forces acting on the microelement body.

The component formula of the momentum conservation equation in the x-direction is:

$$\frac{\partial(\rho u)}{\partial t} + div(\rho u u) = -\frac{\partial p}{\partial x} + \frac{\partial \tau_{xx}}{\partial x} + \frac{\partial \tau_{yx}}{\partial v} + \frac{\partial \tau_{zx}}{\partial z} + F_x$$
(6)

The component formula of the momentum equation in the y-direction is:

$$\frac{\partial(\rho v)}{\partial t} + div(\rho v \mathbf{u}) = -\frac{\partial p}{\partial y} + \frac{\partial \tau_{xy}}{\partial x} + \frac{\partial \tau_{yy}}{\partial y} + \frac{\partial \tau_{zy}}{\partial z} + \mathbf{F}_{y}$$
(7)

The component formula of the momentum equation in the z-direction is:

$$\frac{\partial(\rho w)}{\partial t} + div(\rho w u) = -\frac{\partial p}{\partial z} + \frac{\partial \tau_{xz}}{\partial x} + \frac{\partial \tau_{yz}}{\partial y} + \frac{\partial \tau_{zz}}{\partial z} + Fz$$
(8)

Where the pressure on the p —— fluid microelement

 τ_{xx} τ_{xy} τ_{xz} , —— The component of the viscous stress acting on the surface of the microbody τ F_x F_y F_z , —— The volume force of the microelement, the volume force generated by gravity is... F_x = F_y = 0 F_z = $-\rho g$

3. Study on the Flow Field and Separation Efficiency of the Vertical Centrifuge

3.1. Geometric Modeling

In this section analyzes the internal flow field and the separation efficiency of the vertical separator, the method used in this chapter is calculated based on fluent, using the Euler -- Lagrangian method, the water phase is Euler fluid, the particles in water are the Lagrangian particles, the interaction force between water and particles, calculate the internal flow field and separation efficiency of the separator under different working conditions. The following introduces the whole analysis and research process in detail:

After the boolean operation and the extraction of the fluid domain, the geometric model of the extraction fluid is shown as follows, and the geometric size is shown in the second chapter, which will not be repeated here:

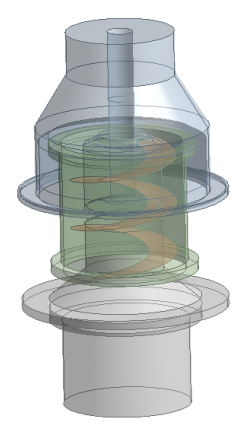


Fig 1. The geometric model of the extraction fluid

3.2. Grid Quality Evaluation Method

(1) Orthogonal quality

For the determination of grid quality, it is mainly composed of several concepts, orthogonality, distortion, and maximum and minimum ratio. In general numerical analysis, we introduce a grid quality standard, 0 is the worst, and 1 is the best. In the whole process, we should make the grid as close as possible to 1.

$$\frac{A_{i} \cdot f_{i}}{|\overrightarrow{Ai}||\overrightarrow{f_{i}}|} \cdot \frac{A_{i} \cdot c_{i}}{|\overrightarrow{Ai}||\overrightarrow{c_{i}}|}$$

$$(9)$$

For two-dimensional triangles are calculated from each edge i:

Where, Ai- -the normal vector of the face, fi- -is the center of mass of the vector to the face, ci- also a vector from the center of mass to the center of the adjacent unit, and ei- -is a vector from the center of mass of a face to the center of the edge. Figure 2 presents a schematic diagram of the orthogonal mass of the grid.

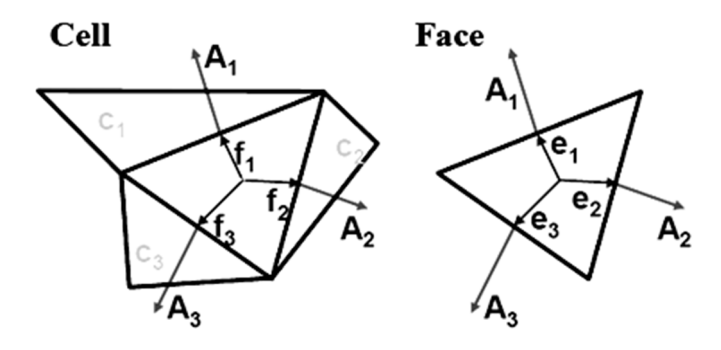


Fig 2. Schematic of the grid orthogonal mass

The following figure shows the main evaluation criteria of grid quality, in which near 1 is good grid, and close to 0 is poor grid quality. In the process of division, the grid area 1 should be made as far as possible, and the minimum requirement of the mainstream solver is more than 0.1. Generally speaking, the mass of the tetrahedral mesh is less than that of the hexahedral mesh, but in the division process, the hexahedral mesh division needs more time. Because the tetrahedral algorithm is more mature, the division time does not need to take up too much.

Inacceptable	Bad	Acceptable	Good	Very good	Excellent
0-0.001	0.001-0.14	0.15-0.20	0.20-0.69	0.70-0.95	0.95-1.00

Fig 3. Quality measures of orthogonal grids

Grid skew is a commonly used method to evaluate grid quality. There are two methods to evaluate grid quality for different types of grids:

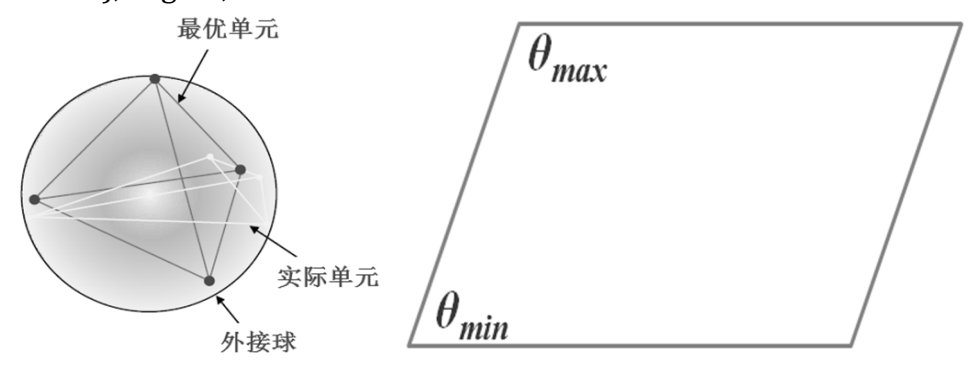
1) Skew is determined by unit dimensions:

Note: This method is the only case for triangular and tetrahedral meshes.

2) The skew is determined by the cell Angle

skew= max
$$\left[\frac{\theta_{\text{max}} - \theta_e}{180 - \theta_e}, \frac{\theta_e - \theta_{\text{min}}}{\theta_e}\right]$$
 (11)

 θ_e Where, -standard geometric decent angle (60° for triangle or tetrahedron, 90° for quadrangle and hexahedral mesh), degree;



(A) Determination by cell size (b) determination by cell angle

Fig 4. Schematic diagram of the skew degree

For skew, if it is a triangle, the positive triangle grid quality is the best, the rest is poor, the greater the Angle difference, the mass is worse, if it is a quadrilateral, square or rectangle mass is the best, the greater the other Angle deviation, the worse the mass.

Excellent	Very good	Good	Acceptable	Bad	Inacceptable
0-0.25	0.25-0.50	0.50-0.80	0.80-0.94	0.95-0.97	0.98-1.00

Fig 5. Measurement standard chart of grid skew

3) Longdness ratio

Wth ratio = δ x / δ y, aspect ratio equal to 1 is the best unit, generally should not exceed 5; suitable for quadrangle grid, see Figure 6.



Fig 6. Schematic representation of the aspect ratio

3.3. Model Grid Quality Evaluation

The grids created in this chapter are mainly triangular grid and quadrangle grid. The quality of the grid created in this chapter is detected through the Mesh quality check function in the Ansys ICEM module. The following results can be obtained by evaluating the grid by the above evaluation criteria.

Table 1. Quality Assessment Table of grid cells

Evaluation method	The worst grid unit	Evaluation results
Orthogonal mass	0.92639	qualified
skewness	0.39654	qualified
length-width ratio	3.68732	qualified

It can be seen from the above table that the grid quality of the model meets the required value range and can meet the requirements of subsequent calculation.

3.4. Grid Division

Using a tetrahedral mesh of the entire geometric domain, Using the global control and layout encryption mode, Setup by setting the part mesh setup, The following figure shows the distribution law of all grids in the geometric domain and the grid distribution of the geometric domain profile, The grid-independent analysis was performed during the grid partition process, Considering the influence of grid quantity and grid quality on the calculation results, For the existing computing domain, The number of divided grids was 790,000,1.56 million, Grid number of 2.77 million, 5.62 million and 12.08 million grids, The inlet pressure was used as the criterion to determine whether the grid converges.

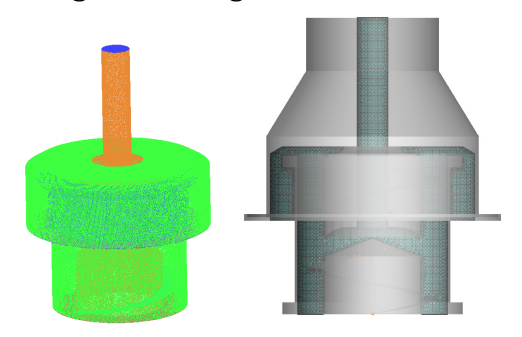


Fig 7. The distribution law of all the grids in the geometric domain and the grid distribution of the contour of the geometric domain

The figure above figure shows the grid distribution in the entire region of the fluid, and the results are as follows:

Table 2. The results					
Grid number (ten thousand)	Average inlet pressure (Pa)				
79	365.59				
156	499.65				
277	512.36				
562	511.57				
1208	512.89				

Table 2. The results

Table in the data can get, when the grid number is 2.77 million, entrance average pressure tends to be stable, the calculation condition using the speed inlet, pressure outlet, the speed entrance speed size is 1 m/s, for pure water, from the perspective of calculation accuracy and calculation speed, the subsequent all grid scale choose the scale of the grid, draw the curve is as follows:

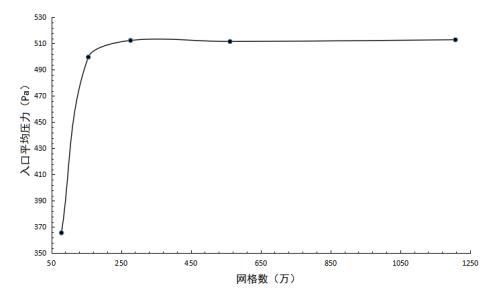


Fig 8. Draw the curve

The pressure curve is from small to large, gradually tends to stabilize, and the grid scale of 2.77 million is selected to have the highest efficiency to solve the problem.

3.5. Solution Settings

The fluent solver to solve the whole problem, which handles the whole problem in the form of steady-state pressure base, the entrance of speed inlet, two outlet, one for water phase outlet, one for particle solid outlet, pressure outlet, considering for relative atmospheric pressure 0Pa, the sliding grid part consider the working speed, 0.1 rad/s, iterative algorithm using SIMPLE algorithm, discrete format is as follows:

Pressure item second order

Momentum item Second order windward

Turbulence kinetic energy term First-order windward

Turbulence diffusivity term First-order windward

Table 3. Discrete format

Over the whole process, the results were extracted after calculating convergence, considering a residual curve of 10e-3.

4. Discussion of Results

The results are discussed on the basis of calculation convergence, mainly from the streamline, velocity, pressure and the separation efficiency of particles. The calculation results are as follows:

(1) Streamline

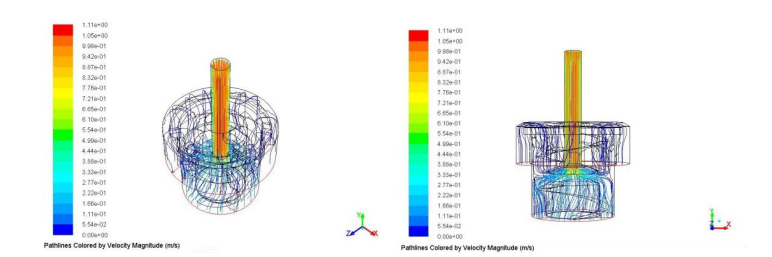


Fig 9. The streamline distribution of the entire computing domain

Above is the streamline distribution of the entire computing domain, sand containing fluid from the inlet into the equipment, after the shell, drum, from the streamline, some outflow from the upper outlet of the lower outlet, the streamline distribution is more uniform, in the 360 degrees on the streamline density, proof that the structure design is reasonable, the processing efficiency is high, the inlet speed of 1 m / s, the calculation results, the maximum flow rate in the middle position, reach 1.1 m/s, after the lower support, fluid separated from all around.

(2) Speed

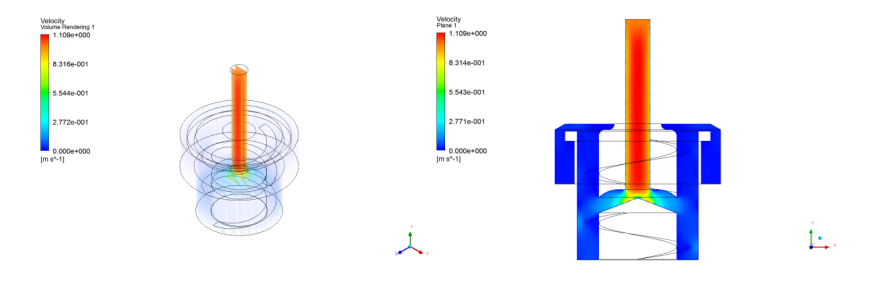


Fig 10. The speed distribution under the working condition

Above is the speed distribution under the working condition, the calculation results, the maximum speed in the middle of the inlet pipe, the speed of the separator side is low, according to the particle settlement critical rate, the lower the rising velocity, particle settlement efficiency of the highest, due to the effect of the spiral drum, at the particle outlet, has a large speed, conducive to the exit of the particles.

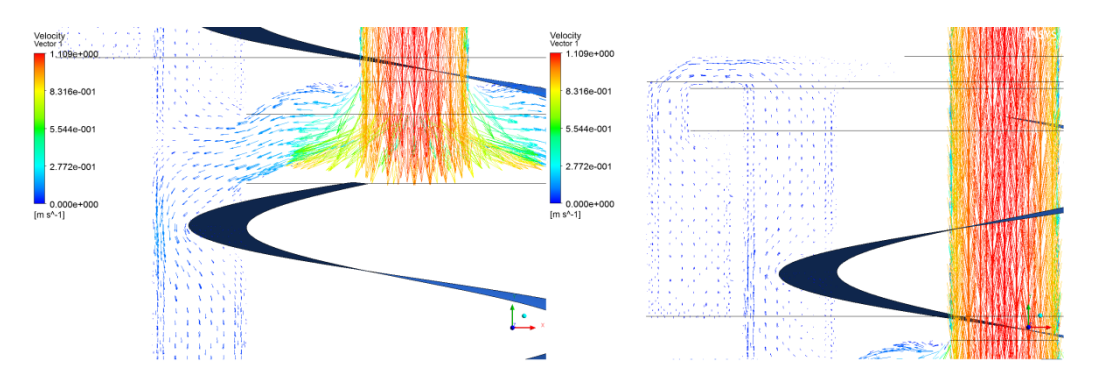


Fig 11. The velocity vector distribution at the whole section

The above figure shows the velocity vector distribution at the whole section, focusing on the comparison of the velocity vector at the upper water outlet and the lower end. The calculation results show that the fluid flow rate at the lower end is about 0.2 m/s, and the upper end is small, 0.15m / s. From the velocity vector results, the whole calculation domain has a reasonable layout and has good separation efficiency.

(3) Pressure | Pressure | 1,397e+003 | 1,386e+003 | 1,386e+003 | 1,386e+002 | Pal | 1,22e+002 | 1,266e+002 | Pal | 1,22e+002 | Pal | 1

Fig 12. The entire computing domain pressure distribution cloud map

Above is the entire computing domain pressure distribution cloud map, the maximum pressure appears at the bottom of the entrance at the bottom of the support at the end of the terminal, the maximum pressure for several reasons, the first for inlet fluid in the large direction, forming a large point pressure, drum rotation here, and formed the fluid pressure accumulation, so the outlet pressure relatively uniform distribution, outlet pressure distribution can effectively ensure the speed of particles and fluid is small, improve the separation efficiency.

(4) Separation efficiency

In this condition, the injection amount of particles is $0.01 \, \text{kg}$ / s, the particle size is 1mm, and the density is $1500 \, \text{kg/m3}$. The internal calculation domain is calculated by using the surface release, and the total number of particles is 504. By counting the number of particles at the water phase outlet and the separation efficiency of the vertical separator is discussed. The calculation results are as follows:

The above figure shows the flow track of the particles inside the equipment. In the above figure, the particles are spread to the periphery of the support along the support, and lead the

downward movement under the joint action of gravity and downward flow, and a few particles flow out from the upper end. The separation efficiency is 84.52%.

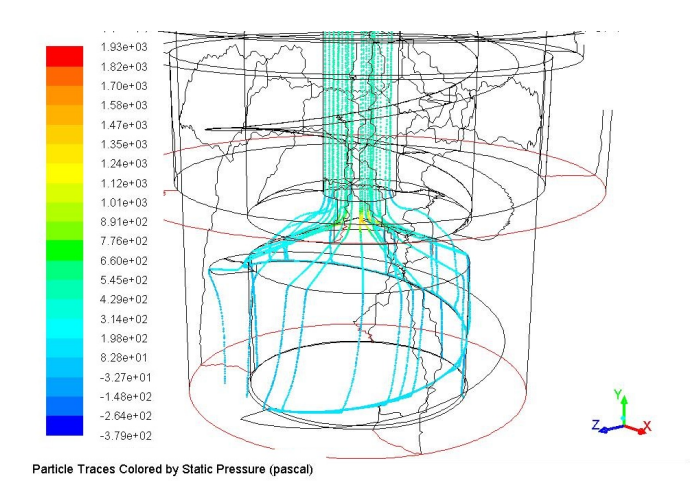


Fig 13. The flow track of the particles inside the equipment

Table 4. Calculation results of separation efficiency of vertical separator

The entrance release	Water export	Particle export		
504	78	426		

(5) Multivariate analysis

The internal flow field and separation efficiency of vertical separator with flow rate of 1 m/s, particle injection volume of 0.01kg / s, rotation speed of 0.1 rad/s, particle size of 1mm and particle density of 1550 kg/m3 are analyzed and discussed. The following separation efficiency of vertical separator is analyzed and studied by univariate method, and the calculation results are summarized as follows:

Table 5. The calculation results

Water flow rate (m/s)	0.8	1	1.2	1.5
Parlet injection (kg / s)	0.01	0.01	0.01	0.01
Drum rotation speed (rpm)	3000	3000	3000	3000
Particle size (mm)	1	1	1	1
Particle density (kg/m3)	1550	1550	1550	1550
separation efficiency	86.64	84.52	81.23	80.07

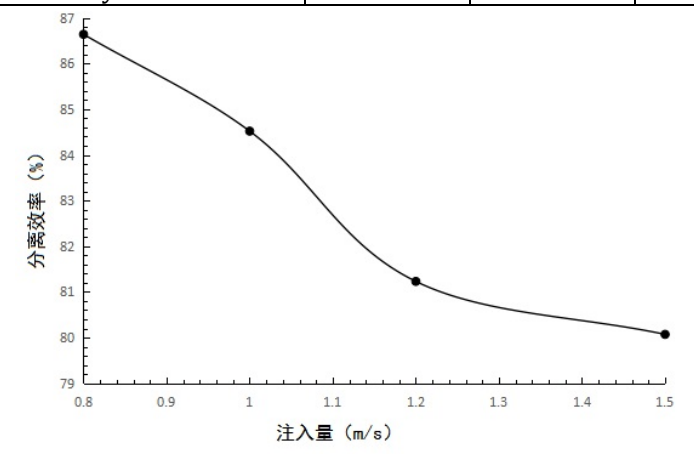


Fig 14. Graph of separation efficiency and injection volume

The result show that the separation efficiency is gradually reduced with the increase of injection, and the separation efficiency of particles is greatly affected in the calculation range.

Table 6. The Calculation result

Water flow rate (m/s)	1	1	1	1
Parlet injection (kg / s)	0.005	0.01	0.015	0.02
Drum rotation speed (rpm)	3000	3000	3000	3000
Particle size (mm)	1	1	1	1
Particle density (kg/m3)	1550	1550	1550	1550
separation efficiency	84.98	84.52	84.22	81.89

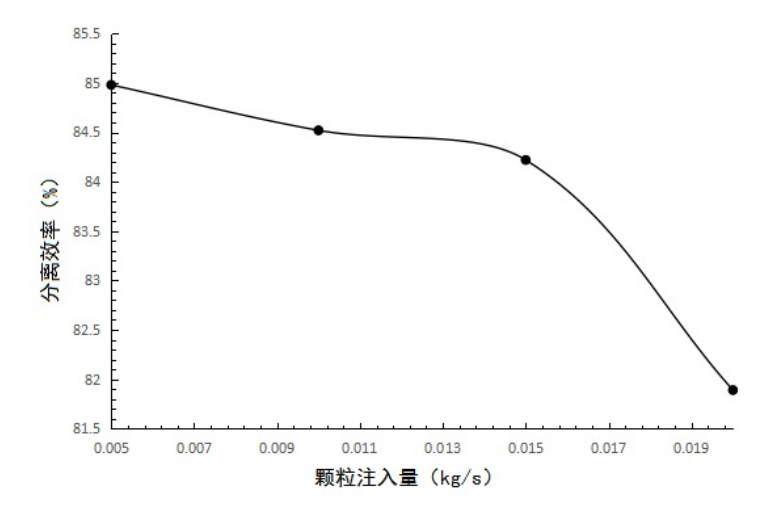


Fig 15. Graph of separation efficiency and particle injection volume

In the calculated range, the injection of particles has little influence on the separation efficiency, and the larger the injection of particles decreases the separation efficiency.

Table 7. The Calculation result

Water flow rate (m/s)	1	1	1	1
Parlet injection (kg / s)	0.01	0.01	0.01	0.01
Drum rotation speed (rpm)	2500	3000	3500	4000
Particle size (mm)	1	1	1	1
Particle density (kg/m3)	1550	1550	1550	1550
separation efficiency	81.02	84.52	86.58	83.15

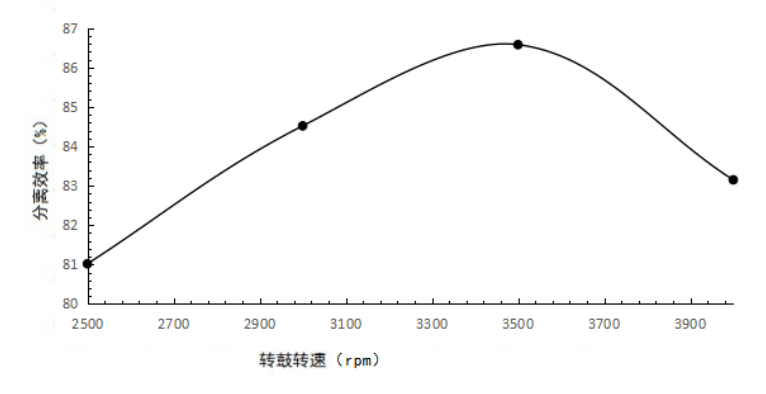


Fig 16. Graph of separation efficiency and drum speed

The calculation results show that there is an optimal value in the drum speed, and the higher and lower drum speed is not conducive to the improvement of the separation efficiency, and the drum speed has a great influence on the whole separation efficiency.

Table 6. The Galculation result						
Water flow rate (m/s)	1	1	1	1		
Parlet injection (kg / s)	0.01	0.01	0.01	0.01		
Drum rotation speed (rpm)	3000	3000	3000	3000		
Particle size (mm)	0.5	1	1.2	2		
Particle density (kg/m3)	1550	1550	1550	1550		
separation efficiency	81.02	84.52	86.58	83.15		

Table 8. The Calculation result

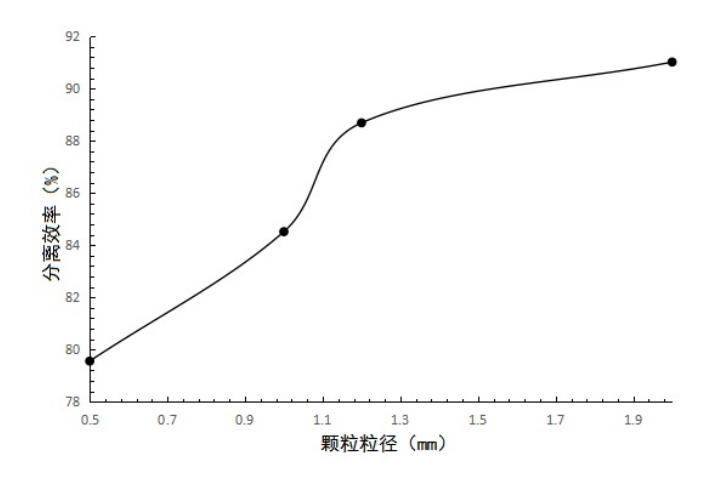


Fig 17. Graph of separation efficiency and particle size

The effect of particle size on the calculation is large, and the separation efficiency increases as the particle size increases.

5. Conclusion

Through multivariate analysis, the separation efficiency is gradually reduced with the increase of the injection amount, and the injection amount has a great influence on the separation efficiency of the particles within the calculated range. The injection amount of particles has little influence on the separation efficiency, and the larger the injection amount, the lower the separation efficiency. There is an optimal value in the drum speed, and the higher and lower drum speed are not conducive to the improvement of the separation efficiency, and the drum speed has a great influence on the whole separation efficiency. The effect of particle size on the calculation is large, and the separation efficiency increases as the particle size increases.

References

- [1] Lu Ning, research on the distribution characteristics of solid-liquid two-phase flow particles in a high-speed centrifuge, 2017, Xi'an University of Technology, p. 75.
- [2] Zhou Gaohua, design and study of three horizontal spiral unloading settling centrifuge, 2005, Sichuan University p. 103.
- [3] Chen Jitao, fault analysis and solution of horizontal spiral centrifuge for petrochemical industry Chemical Design Communication, 2018.44 (07): page 79.
- [4] Zhou Jin et al., using the double rotor horizontal screw centrifuge model with power test, Journal of Zhejiang University (Engineering edition), 2019.53 (02): page 241-249.

- [5] Wang Wentao, Analysis and prediction of erosion and wear of overcurrent rotating parts of vertical centrifuge, 2014, Hunan University of Technology, p. 73.
- [6] S., Z.and X.W.X., UNBALANCE IDENTIFICATION AND FIELD BALANCING OF DUAL ROTORS SYSTEM WITH SLIGHTLY DIFFERENT ROTATING SPEEDS. Journal of Sound and Vibration, 1999. 220(2).
- [7] Jiao Guowang, Zhang Jianrun and Wang Bin, Analysis of Mechanical Manufacturing and Automation, 2010.39 (01): Page 22-24 + 41.
- [8] Liu Jianli, LW-450N Research Research, 2015, Zhejiang University of Technology, p. 51.
- [9] Jing Jidong, development of key structures of horizontal spiral centrifuge, 2021.36 (12): Pages 143-144 + 174.
- [10] Qiu, B.H., J.L.Qing and J.Z.Sheng, Three Dimensional Numerical Simulation of Solid-Liquid Separation of Horizontal Spiral Sedimentation Centrifuge. Advanced Materials Research, 2013. 2203 (634-638).
- [11] Patents; Patent Application Titled "Fully Jacketed Screw Centrifuge" Published Online.Politics & Government Week, 2015.
- [12] GEA Mechanical Equipment GmbH; Patent Issued for Solid-Bowl Screw Centrifuge with Outlet Openings for Partial and Residual Emptying of the Drum. Journal of Engineering, 2013.
- [13] GEA Mechanical Equipment GmbH; Patent Issued for Method For Monitoring A Screw Centrifuge To Identify Dynamic Changes In Relative Angular Offset Between An Output Shaft And A Transmission Input Shaft (USPTO 10,744,518). Journal of Engineering, 2020.
- [14] Guorui, Z., T.Wei and Y.Yang, Experimental and Numerical Study of the Solid Concentration Distribution in a Horizontal Screw Decanter Centrifuge.Industrial & Engineering Chemistry Research, 2013. 52(48).
- [15] Flottweg SE; Patent Issued for Solid-Bowl Screw Centrifuge Having An Energy Recovery Device (USPTO 10,105,715). Journal of Engineering, 2018.
- [16] Tian, et al., Multivariate statistical analysis of the quality of apple juice to integrate and simplify juice industrial production technologies.CyTA Journal of Food, 2018. 16(1).
- [17] Lu Fangfei, finite element analysis of the screw conveyor, 2020, Shenyang University of Technology, p. 59.